1-1-2013

Supramolecular step in design of nonlinear optical materials: Effect of pi ... pi stacking aggregation on hyperpolarizability

Kyrill Yu Suponitsky
University of Central Florida

Artëm E. Masunov
University of Central Florida

Supramolecular step in design of nonlinear optical materials: Effect of $\pi...\pi$ stacking aggregation on hyperpolarizability

Cite as: J. Chem. Phys. **139**, 094310 (2013); https://doi.org/10.1063/1.4819265
Submitted: 24 April 2013 . Accepted: 12 August 2013 . Published Online: 06 September 2013

Kyrill Yu Suponitsky, and Artëm E. Masunov

Supramolecular step in design of nonlinear optical materials: Effect of $\pi \ldots \pi$ stacking aggregation on hyperpolarizability

Kyrill Yu Suponitsky[1,a),b)] and Artëm E. Masunov[2,a),b)]
[1]*NanoScience Technology Center, University of Central Florida, Orlando, Florida 32826, USA and A. N. Nesmeyanov Institute of Organoelement Compounds, Russian Academy of Sciences, 28, Vavilov Street, B-334, Moscow 117813, Russia*
[2]*NanoScience Technology Center, Department of Chemistry, and Department of Physics, University of Central Florida, Orlando, Florida 32826, USA*

(Received 24 April 2013; accepted 12 August 2013; published online 6 September 2013)

Theoretical estimation of nonlinear optical (NLO) properties is an important step in systematic search for optoelectronic materials. Density functional theory methods are often used to predict first molecular hyperpolarizability for compounds in advance of their synthesis. However, design of molecular NLO materials require an estimation of the bulk properties, which are often approximated as additive superposition of molecular tensors. It is therefore important to evaluate the accuracy of this additive approximation and estimate the extent by which intermolecular interactions influence the first molecular hyperpolarizability β. Here we focused on the stacking aggregates, including up to 12 model molecules (*p*NA and ANS) and observed enhancement and suppression of molecular hyperpolarizability relative to the additive sum. We found that degree of nonadditivity depends on relative orientation of the molecular dipole moments and does not correlate with intermolecular interaction energy. Frenkel exciton model, based on dipole-dipole approximation can be used for qualitative prediction of intermolecular effects. We report on inaccuracy of this model for the molecules with long π-systems that are significantly shifted relative to each other, when dipole-dipole approximation becomes inaccurate. To obtain more detailed information on the effect of intermolecular interactions on β we proposed electrostatic approach which accounts for the mutual polarization of the molecules by each other. We measure the induced polarization of each molecule in the aggregate by the charge of its donor (or acceptor) group. The proposed approach demonstrates linear correlation β^{FF} vs β^{elm} (estimated by finite field theory and electrostatic model, respectively) and allows decomposition of the hyperpolarizability for a molecular aggregate into separate molecular contributions. We used this decomposition to analyze the reasons of deviation of aggregate β from additivity, as well as the cooperative effect of intermolecular interactions on hyperpolarizability for stacks of growing size. In cases of positive cooperativity (enhancement), we found 6–8 molecules to be necessary to reach the asymptotic limit. In more frequent cases of negative cooperativity two opposite factors play role. The first one consists of direct lowering of β due to repulsive dipole-dipole interactions. The second factor is originated in a decrease of molecular dipole moments, which in turn leads to a decrease of dipole-dipole repulsion, and therefore increases β. For strong intermolecular repulsive dipole-dipole interactions these effects nearly cancel each other. In such cases the trimers and even dimers are sufficient to reach the asymptotic limit of the infinite stacks. Based on the observed trends we estimated non-additive correction to β for well known NLO crystals NPAN and MNMA. In the case of NPAN, stacking effect on molecular hyperpolarizability represents the leading component of the crystal packing effect and improves the agreement between calculated and experimental data which is further improved when frequency dependence is taken in account. © *2013 AIP Publishing LLC*. [http://dx.doi.org/10.1063/1.4819265]

I. INTRODUCTION

Materials that possess strong nonlinear optical (NLO) properties hold a great promise for the applications in all-optical and optoelectronic technologies.[1–4] Extensive investigations in this field produced many different classes of organic and organometallic compounds, as well as efficient methods for prediction of NLO properties.[5–10] Rational design of organic NLO materials can be divided into two steps:[1(c),5,8] are references (i) molecular design, followed by (ii) supramolecular design of material, composed of these molecules. This material can be either crystalline, or thin film, or polymer. Search for molecules with optimal molecular structure that give rise to the high molecular nonlinearities as well as numerous theoretical and experimental studies of molecular optical properties resulted in a detailed understanding of the origin of the molecular properties necessary for a development of new NLO materials.[4,5,8,11,12] The π-conjugated molecules endcapped with donor (D) and acceptor (A) substituents allow easy electronic redistribution

[a)]K. Yu. Suponitsky and A. E. Masunov contributed equally to this work.
[b)]Electronic addresses: kirshik@yahoo.com and amasunov@ucf.edu

in the molecule upon excitation by an applied electric field thereby giving rise to high molecular (hyper)polarizabilities. An appropriate choice of the length and composition of a π-conjugated bridge and the strength of D/A groups allows to design molecules with optimal trade-off between hyperpolarizability and optical transparency.[13–16]

The second, supramolecular step in material design is taken less frequently. Rare examples of crystalline material investigation were presented by calculation of hyperpolarizability for small, highly symmetric crystals of semiconductors and urea.[17–19] These studies were based on analytic derivatives technique, implemented into the CRYSTAL program to allow calculation of the optical properties within periodic boundary conditions. Another method of hyperpolarizability prediction was applied to urea and organic *para*-nitrophenolates.[20] It was based on the calculations of periodical structures in the presence of the finite electric field using Berry phase approach, as implemented in CPMD.[21] The predictions for the entire crystal do not provide an opportunity to analyze the separate factors (such as molecular orientation), affecting to resulting value, however.

Common way of calculation is based on assumption that the properties of the material are well represented by the tensorial sum of molecular properties (additive approximation), while the effect of intermolecular interactions is completely neglected (this is known as oriented gas model).[22,23] This approximation is sometimes justified by the large ratio of intra- to intermolecular interaction energies (~2–3 orders of magnitude),[24] and it yields qualitative agreement with experiment in some cases.[5,25] However, to obtain quantitative predictions one needs to take intermolecular effects into account.

Intermolecular interaction energy is determining not only thermodynamics, but many other crystalline properties, including magnetic and optical properties. For instance, the luminescent properties in a certain class of organometallic compounds were shown to depend on the nature and energy of intermolecular interactions.[26] Even though the early applications of the oriented gas model included effects of the crystalline environment in the form of the point charges,[27] many recent applications of this model[28] are based on the assumption that intramolecular interactions are much stronger than intermolecular interactions and therefore one can completely neglect intermolecular interactions in NLO predictions. It is also believed that oriented gas model is a better approximation for crystals stabilized by weak van der Waals interactions, than for crystals stabilized by hydrogen bonds (that are much stronger).

In this contribution we will show that at least for the interactions of the same nature the interaction strength does not necessarily correlate with effect on hyperpolarizability. We study this effect for several molecular clusters, representing π-stacks, typical for the crystals of the conjugated chromophores. When the stacks are present, the nearest neighbors for each molecule are found within the same stack, while the other intermolecular interactions are necessarily realized over considerably larger distances. Consideration of other types of interactions, such as H-bonds is the subject of further investigation and this research is ongoing.

The effect of the molecular environment on the first hyperpolarizability (β) is clearly non-negligible. It becomes apparent from comparison of molecular hyperpolarizabilities in solution and gas phases.[15,29] In more polar solvents the higher the β value is observed. Other factors, such as aggregation and H-bonding can also contribute.[30–33] A nonadditive enhancement of β of push-pull chromophores linked through σ-bridge has also been reported.[34,35] At the same time nearly parallel arrangement and side-to-side interaction of the chromophores in macrocyclic trimeric bundle was reported to have β that is 20% decreased in comparison with the additive model.[36] The hypsochromic excited state shift and diminished difference between the ground and excited state dipole moments were identified as the reason for this nonadditivity. Similar results were obtained for hyperpolarizability of D/A-dendrimers. The conjugated components of these molecular systems are held together by σ-bonds between the chromophore units. In addition, there are parallel side-to-side and linear head-to-tail through-space interchromophore interactions, that give rise to lowering and enhancement of β, respectively.[37,38] The effect of nonbonding $\pi\ldots\pi$ interactions on β was observed in calixarenes,[39,40] paracyclophanes,[41,42] and other branched molecules, where two (or more) aromatic fragments are in close proximity to each other.[43–46]

An early study on *para*-nitroaniline (*p*NA)[47,48] revealed that hyperpolarizability of the $\pi\ldots\pi$ stacked dimers significantly deviates from an additive model: decrease of β by 18% for the face-to-face dimer was found for interplanar separation distance near 3.5 Å (sum of van der Waals radii of two carbon atoms[49]). Pulling the monomers apart increases the hyperpolarizability to nearly twice of its monomeric value and brings it in agreement with additive model at distances over 9 Å. Similar result (decrease by 31%) was obtained for 2-methyl-4-nitroaniline (MNA) stacking dimer.[50] Deviation from the additive model was also reported for D/A-substituted porphyrin,[51] azobenzene and plyene[52] dimers. At the same time, H-bonded head-to-tail dimer of *p*NA,[47,53,54] HCN,[55] and other D/A-substituted benzenes[56] demonstrate sizable enhancement of hyperpolarizability.

Many crystal structures of NLO compounds are composed of the molecules which contain benzene or other aromatic rings as well as π-conjugated bridges.[57] As a result, their crystal structures are usually stabilized by $\pi\ldots\pi$ stacking interactions, as well as H-bonding and other noncovalent interactions. The effect of intermolecular interactions on hyperpolarizability in the crystal can be studied computationally by supermolecule approach, using molecular aggregates of increasing size.[58,59] For example, in Refs. 60 and 61 two types of urea clusters were taken from the crystal structure: (i) linear H-bonded chains and (ii) stacks along (0-11) direction. While the interactions in the chain make a significant contribution to the total intermolecular energy, the interactions in the stack were rather weak.[62] Hyperpolarizability of H-bonded chains demonstrates significant deviation from additivity (in agreement with earlier studies[63,64]), while specific monomeric value (β_n/n) in the stack remains nearly constant. At the same time, the aggregate built from 9 unit cells demonstrated insignificant deviation of β_{abc} from the one predicted by oriented gas model.[65] Apparently, this is result of

cumulative effect when nonadditivity of antiparallel H-bonded chains along *c* crystallographic direction cancel each other. Similar results were obtained for estimation of crystal nonlinear susceptibility of the 3-methyl-4-nitropyridine-1-oxide (POM).[66] Only nonvanishing tensor component β_{abc} is nearly constant in aggregates along *a* axis, it is increased by 11% upon growing of an aggregate size along *b* axis and decreased by 21% along *c* axis. In the case of MNA, on the other hand, the effect of molecular environment on β is significant. The studies report[67,68] 5-fold increase along *a* axis, and 28% and 49% decrease along *b* and *c* axes, respectively. Overall, this leads to nearly doubling of NLO susceptibility compared to the oriented gas model. Increase in NLO susceptibility by 15% relative to oriented gas model was also predicted in crystals of *meta*-nitroaniline (*m*NA).[69]

The results summarized above suggest that the accuracy of the oriented gas model varies and it can be used only for qualitative description of crystal susceptibility. In order to reveal the reasons why it errs, we present here a systematic study of the effect of intermolecular interactions on molecular hyperpolarizability. In the present work we investigate $\pi\ldots\pi$ stacking interactions, while the study of hydrogen bonding effect will be reported elsewhere. Two main topics are considered: (i) the orientation effect of the closest molecular neighbors on hyperpolarizability and (ii) the cooperative effect. While effect of orientation can be studied on dimeric structures, the overall effect of molecular packing typically reaches the asymptotic value only in larger aggregates. For instance, H-bonding in chains in 1,3-cyclohexadione can be adequately predicted by calculation of the chain hexamers,[70,71] while 8 molecules in the chain are necessary for accurate description of H-bonding in urea.[72] The crystal structure of acetic acid was reproduced by calculation of 3-dimensional aggregate built up of 36 molecules.[73,74] Similar conclusions on cooperative effect of intermolecular interactions on the structure and stability of aggregates were also made for other systems.[75–79] Even in the case of POM and urea, nearly additive total values of β_{abc} are the combination of the opposite cooperative contributions: negative and positive deviation from additivity in different crystallogrphic directions. In the present work, cooperative effect is studied in stacking aggregates of increasing size (up to 12 molecules).

Another important question is the choice of appropriate theory level.[80,81] The size of systems under study does not allow using highly sophisticated correlated methods such as MP2 or coupled cluster theory. Fortunately, development of new DFT functionals and their validation for prediction of linear and nonlinear optical properties[10,82–97] have made DFT a promising tool. It is capable to handle systems of relatively large size (long and branched conjugated molecules or molecular aggregates). Development of range-separated hybrid functionals allows to partly correct for self-interaction error (SIE)[98–104] and results in significantly improved predictions of molecular NLO properties.[105–116] Another way to reduce SIE is to use the global hybrid functionals with the increased fraction of HF exchange.[84,117–121] Recently we have shown that M05-2X functional which contains 56% of HF exchange provides the improved accuracy and can be used to estimate molecular hyperpolarizability.[122] An added advantage of this functional for study molecular aggregates is that it was purposely developed to correctly describe the energy of the mid-range nonbonded interactions.[123–126]

II. COMPUTATIONAL DETAILS

When a molecule is placed in the electric field of the strength *E*, its dipole moment can be expanded in the Taylor series by the orders of the field strength:

$$\mu_i = \mu_i^0 + \alpha_{ij}\cdot E_j + \beta_{ijk}\cdot E_j\cdot E_k + \gamma_{ijkl}\cdot E_j\cdot E_k\cdot E_l + \cdots, \tag{1}$$

where $\mu_i{}^0$ is the dipole moment of the unperturbed molecule (permanent dipole moment), α_{ij} is the linear polarizability, β_{ijk} and γ_{ijkl} are the first and second hyperpolarizabilities, respectively. The first hyperpolarizability tensor components are obtained as the second derivatives of the dipole moment with respect to the applied field or as the negative third derivatives of the energy (*W*) with respect to the applied filed:

$$\beta_{ijk} = -\left.\frac{\partial^3 W(E)}{\partial E_i \partial E_j \partial E_k}\right|_{E=0}. \tag{2}$$

Gaussian 2003 suite of programs was used in this study to obtain all the numerical results.[127] In this code the static hyperpolarizability can be evaluated as the third derivative of the energy (taken numerically with the finite field (FF) approach with the use of Polar = EnOnly keyword). The dynamics hyperpolarizabilities were also evaluated for selected systems by analytical derivatives, using CPHF = RdFreq keyword in Gaussian 2009. Vectorial part of β was calculated from tensor components β_{ijk} as

$$\beta_{vect} = \left(\beta_x^2 + \beta_y^2 + \beta_z^2\right)^{1/2}, \quad \text{where}$$
$$\beta_j = \frac{1}{3}\sum_{i=1}^{3}(\beta_{jii} + \beta_{iji} + \beta_{iij}),\ i, j = x, y, z. \tag{3}$$

The crystalline nonlinear susceptibility was calculated according to the formula[23]

$$d_{IJK} = \frac{1}{V} f_L \sum_{n=1}^{Z}\left[\sum_{i=1}^{3}\sum_{j=1}^{3}\sum_{k=1}^{3}\cos\theta_{iI}^n \cos\theta_{jJ}^n \cos\theta_{kK}^n \beta_{ijk}\right], \tag{4}$$

where *V* is the unit cell volume, *Z* is a number of molecules per unit cell, $\cos\theta_{iI}^n$ is direct cosines of the angles between molecular and crystal coordinate systems, and f_L is the local field correction factor (set here to be equal to 1 for simplicity), and β_{ijk} tensor components are be taken either for isolated molecules, or for a molecule affected by intermolecular interactions.

Based on reported success of M05-2X functional to describe the energy of intermolecular interactions,[123–126] and on the results of our recent hyperpolarizability study[32,122] we use M05-2X/6-31+G* theory level for the present work. In case of larger molecular aggregates, the diffused basis functions lead to convergence problems and significant increase of the computer time. We have recently shown that basis set reduction from 6-31+G* to 6-31G does not lead to the lack of

accuracy.[121] Therefore, for several stacking aggregates considered in the present work we use M05-2X/6-31G theory level. All charges were calculated with NPA method[128,129] implemented in the Gaussian program. The basis set superposition error (BSSE) effect was studied for selected systems. The BSSE-corrected energies and hyperpolarizabilities were estimated by counterpoise method (Counterpoise keyword in Gaussian 2009).

III. RESULTS AND DISCUSSION

This study is focused on several well-known NLO molecular compounds depicted in Scheme 1. The first two molecules, *p*NA and 4-nitro-4′-aminostilbene (ANS), were used to build stacking aggregates of different types. Two other compounds, 2-methyl-4-nitro-*N*-methylaniline (MNMA) and *N*-(4-nitrophenyl)-*N*-methylamino-acetonitrile (NPAN), were used as the benchmarks. They crystallize in acentric space groups and their NLO properties were studied experimentally.[130,131] The crystal structure of MNMA (space group $Pna2_1$, structural class *mm*2)[130] is composed of H-bonded chains along the *a* axis while in perpendicular direction (parallel to *c* axis) molecules are connected by $\pi\ldots\pi$ stacking interaction (see Figure 1S in the supplementary material[132]). All the other interactions in this crystal belong to van der Waals type. NPAN crystallizes in the space group *Fdd*2, same structural class *mm*2.[133] Unlike MNMA, NPAN molecule does not have acidic hydrogen atoms and does not form H-bonds in the crystal structure. Molecules in the crystal are linked by $\pi\ldots\pi$ stacking interactions along *c* axis (see Figure 2S in the supplementary material[132]), and non-specific van der Waals interactions.

A. Dimers of *p*NA and ANS

We used *p*NA molecules to build the dimer structures, representative of several types of $\pi\ldots\pi$ stacking observed in the crystal structures of aromatic compounds.[134] They are depicted in Scheme 2 and include the molecular orientations in which (i) amino- and nitro-groups are placed over the center of the neighboring the benzene ring, (ii) the benzene rings partially overlap, and (iii) the π-donor amino group of one molecule is located directly above the π-acceptor nitro-group of another one. In all the dimers the molecules are kept parallel to each other, which is frequently observed in the crystal structures[134] (stacks are formed by molecules related by a translation along crystallographic axis). Another common

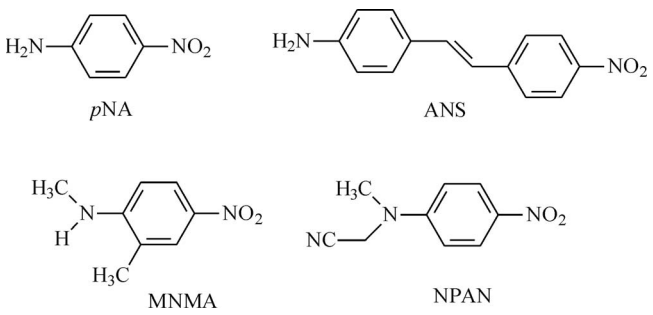

SCHEME 1. Molecules considered in this study.

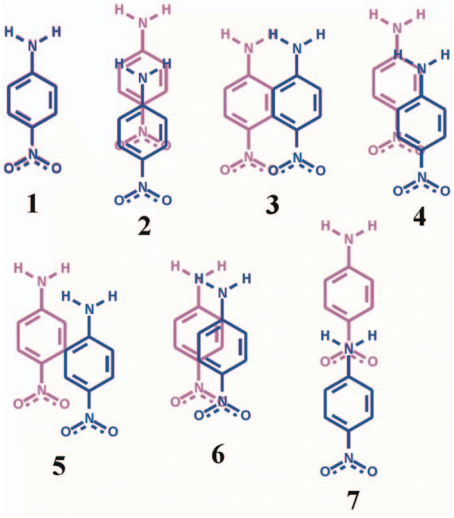

SCHEME 2. Types of *p*NA dimers.

type of $\pi\ldots\pi$ stacking interactions is observed in columns where the neighboring molecules are related by center of symmetry. This arrangement results in cancellation of all hyperpolarizability tensor components and was not considered in this study. We also calculated the interaction energy in face-to-face parallel dimers and found it to be repulsive (Fig. 1).

Although in the crystal *p*NA adopts slightly nonplanar geometry with the planar amino groups rotated out of the plane of the benzene rings,[135] in calculations we used idealized planar optimized geometries of the monomers in C_{2v} symmetry, while the dimer geometry was frozen at various intermolecular distances. The interplanar separation was selected in the range of 3.2–3.6 Å (with 0.05 Å step), which covers typical distances for stacking interactions in the crystals (average carbon…carbon nonbonded separation is 3.5 Å[49]). In the case of Type 7 dimers, the closest contact corresponds to N…N interaction with shorter nonbonded distance 3.22 Å, therefore the range of 2.9–3.4 Å was used for this Type. For each dimer type the optimal intermolecular separation was determined by potential energy scan (Figure 1). All the dimers demonstrated the optimal interplanar separation to be less than sum of nonbonded radii of interacting atoms (with the exception for the face-to-face Type 1, which remained strongly repulsive at all distances). This means that all these types of dimers can in general be observed in the crystal, except for the face-to-face one. Considering that face-to-face Type 1 stacking was extensively investigated in the literature,[47,48] we will not discuss this type any further. Energies of optimal dimers for Types 2–7 are listed in Table I along with their interplanar distances, hyperpolarizabilities, and dipole moments, obtained at M05-2X/6-31+G* theory level.

To test the validity of M05-2X/6-31+G* theory level and the rigid scan approximation, we compared the results for Type 3 dimer with those obtained with the full geometry optimization and zero point energy (ZPE) correction. The comparison shows that both rigid scan and full optimizations lead to similar structures (Figure 3S and Table 1S in the supplementary material[132]). The results obtained with more extended basis set (aug-cc-pVTZ) and correction of β for BSSE

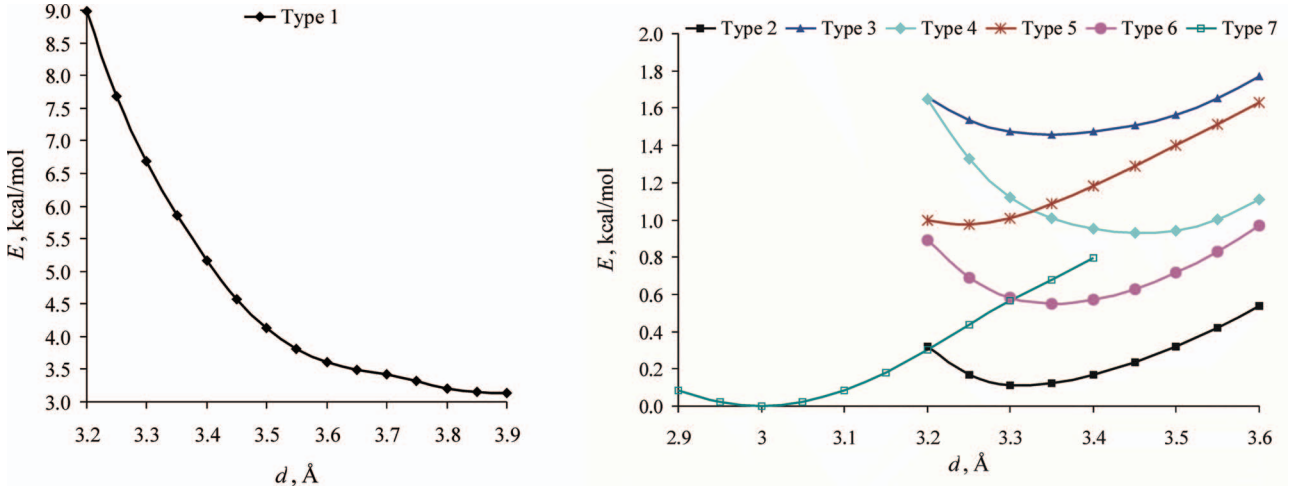

FIG. 1. Dependence of interaction energy (E, kcal/mol) for dimers of different types on interplanar separation (d, Å): Type 1 (left) and Types 2–7 (right). Zero energy corresponds to the equilibrium interaction energy for the most stable dimer (Type 7).

are also shown in the supplementary material[132] (Table 2S). They do not change our conclusions on energy and hyperpolarizability. Absolute values of hyperpolarizability of the *p*NA monomer and dimers of different Types obtained with aug-cc- pVTZ basis set are somewhat smaller (by 7%–12%) relative to those obtained with 6-31+G* basis set. However, the relative deviation of β from the additive model is nearly basis set independent (differences do not exceed 5%). These results are in agreement with our recent study[32] where we had shown that the ratio of hyperpolarizabilities is nearly basis set independent for the molecules of *p*NA and 4-hydroxy-4′-nitrostilbene (HONS).

All the dimers considered (except for Type 7) show hyperpolarizability and dipole moment to be significantly less than sum of monomeric values. This behavior was reported in the literature for other systems where molecules form $\pi \ldots \pi$ stacks.[47,48,50,51] As one can see from the Table I, there is no correlation between interaction energies and hyperpolarizabilities, while linear correlation is observed between β and μ. This fact can be interpreted within Frenkel exciton model which is frequently invoked for a discussion of aggregate optical properties (Scheme 3).[136–138] In this model the overlap between molecular orbitals of two molecules is neglected and their interaction energy is calculated in dipole-dipole approximation. An excited state of the molecule in the dimer is split into two. The splitting energy (ΔE) is defined as[136,137]

$$\Delta E = 2\left[\frac{\boldsymbol{\mu}_{ge}^{(1)}\boldsymbol{\mu}_{ge}^{(2)}}{R^3} - \frac{3(\boldsymbol{\mu}_{ge}^{(1)}\mathbf{R})(\boldsymbol{\mu}_{ge}^{(2)}\mathbf{R})}{R^5}\right], \quad (5)$$

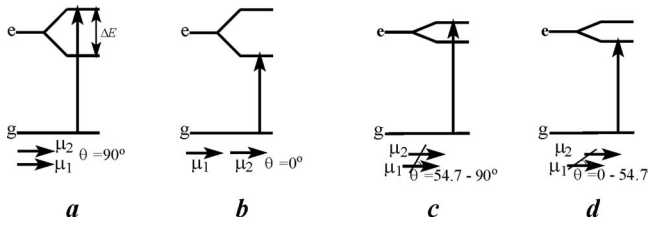

SCHEME 3. Splitting of the excited states upon dimerization as a function of the mutual orientation of their transition dipoles.

where $\boldsymbol{\mu}_{ge}^{(1)}$ and $\boldsymbol{\mu}_{ge}^{(2)}$ are transition dipole moments of two molecules, respectively, R is intermolecular separation. For dimers of identical molecules in parallel orientation (Types 2–7), expression (5) is reduced to

$$\Delta E = 2\mu_{ge}^2 \frac{1 - 3\cos^2\theta}{R^3}. \quad (6)$$

The hyperpolarizability depends on transition energy between ground and excited states E_{ge}^2 according to the expression

$$\beta \sim \Delta\mu \frac{\mu_{ge}^2}{E_{ge}^2}. \quad (7)$$

It therefore depends on intermolecular separation as well as on the angle θ between the line connecting the molecular centers and molecular transition dipole moments (parallel to permanent dipole in *p*NA case). Apparently, whole

TABLE I. Energetic, geometrical, and optical characteristics of *p*NA dimers calculated at M052X/6-31+G* level of theory.

	2 monomers[a]	Type 2	Type 3	Type 4	Type 5	Type 6	Type 7
E (kcal/mol)	3.15	0.11	1.46	0.93	0.98	0.55	0.0
d (Å)	∞	3.30	3.35	3.45	3.25	3.35	3.00
β (au)	2808	2234	1715	1942	1842	1672	3031
Dipole (μ) (D)	15.42	14.57	14.27	14.43	14.32	14.28	15.45

[a]Twice values of energy, hyperpolarizability, and dipole moment of isolated monomer of *p*NA are given for a comparison.

TABLE II. Parameters of Eq. (6) for different types of *p*NA dimers.

	Type 2	Type 3	Type 4	Type 5	Type 6	Type 7
Angle α (deg)	50.0	90.0	60.5	71.2	78.6	28.2
Intermolecular distance R (Å)	4.306	4.136	4.200	4.285	3.634	6.351
$\frac{1-3\cos^2\theta}{R^3}$ (Å^{-3})	-3.0×10^{-3}	14.1×10^{-3}	3.7×10^{-3}	8.7×10^{-3}	18.4×10^{-3}	-5.2×10^{-3}

intermolecular interaction energy obtained from *ab initio* calculations does not necessarily parallel to the dipole-dipole interaction energy. However for weak interactions, contribution of the dipole-dipole forces to the total molecular binding can be significant.

Diagrams *a* and *b* in Scheme 3 correspond to two limiting cases of molecular orientations in dimer ($\theta = 90^\circ$ and $\theta = 0^\circ$, respectively). Changing of angle θ from 90° to 54.7° will result in decrease of the energy splitting to zero, while decrease of θ from 54.7° to 0° will increase this splitting in the reversed order. For these θ values (Scheme 3*c*) the ΔE has a positive sign and dipole-allowed transition occurs from the ground state to higher excited state which results in a decrease of hyperpolarizability. The closer is the θ to 90° the lower is the hyperpolarizability and the higher is the energy splitting ΔE. In the second region of θ values (from 54.7 to 0°, Scheme 3*d*), ΔE is negative and transition occurs to lower excited state thereby resulting in an increase of hyperpolarizability. One can see from Table I that according to finite field calculations, hyperpolarizability is higher than additive sum of two monomers for Type 7 only. At the same time results summarized in Table II demonstrate that Frenkel exciton model predicts two types of dimers (Types 7 and 2) to have enhanced values of β because of negative ΔE. However, at qualitative level, variation of hyperpolarizability upon the way of molecular aggregation is well described in terms of exciton model: β is predicted to increase in the series of Type6 < Type3 < Type5 < Type4 < Type2 < Type7, in agreement with the results reported in Table I.

These numerical results can be explained with even simpler model of electrostatic nature, which is described next. One should note that the term "electrostatic approach" is used rather liberally in application to different problems of physical chemistry, including spectroscopy.[139,140] In particular effect of surroundings was taken into account by electrostatic interaction scheme in prediction of linear susceptibilities of several well-known organic NLO crystals[141,142] and NLO susceptibilities of anil crystals.[143] The novelty of our approach is in the use of atomic charges as reporters of the polarization state of a molecule in an aggregate. In contrast to the exciton model, our model does not consider excited states, but does take into account polarization of the ground state that significantly affects hyperpolarizability values.[13–15] One may consider the ground state of a dimer, where two molecules are mutually polarized (in comparison to their isolated ground states). Charge redistribution associated with this mutual polarization can be quantified in terms of atomic or group charges or their changes relative to the charges in the monomer. Upon positive polarization (increase of dipole moment) donor group will lose and acceptor group will gain electrons, while reverse is true for the negative polarization. At the same time the calculation of hyperpolarizability of the isolated molecule in the presence of external field (command "Field" in the Gaussian program) allows one to obtain relationship between β and the fragment charges. Here we assume for simplicity, that in a dimer molecules are polarized by uniform electric field, induced by the neighbors. This assumption is expected to be accurate only if a size of a molecule is significantly less than intermolecular separation distance. Note that a similar assumption is also made in Frenkel exciton model. Using this relationship (β as a function of charge on D/A groups) one can estimate β of each molecule in the dimer or larger aggregate and identify the origin of hyperpolarizability changes upon aggregation.

To illustrate the proposed model, we applied electric fields of different strengths (from −0.004 to +0.004 a.u. with 0.0005 a.u. step) to *p*NA molecule along the direction of its dipole moment. This range of the field strengths covers fairly well the polarization effects induced by the second molecule in a dimer. The obtained results (see Figures 4S and 5S in the supplementary material[132]) show that in the given range of the field strengths, the dependence is linear for charges of both donor and acceptor groups. Since charge of NO_2 group (q_{NO2}) is slightly more sensitive to changes of the field strength, we used it as an indicator of a molecular polarization. The obtained linear regression is $\beta^{elm} = -12\,742\times q_{NO2} - 2346$. The superscript "elm" refers here to our electrostatic model. These estimates for hyperpolarizability of the dimers and their constituting molecules are presented in Table 3S in the supplementary material[132] and β^{FF} vs β^{elm} is plotted in Figure 2.

The results obtained reveal nearly qualitative agreement between accurate (finite field) βs and approximate β^{elm} values. Only β of Type 6 which should have the smallest value appears slightly higher than that of Type 3. However, the

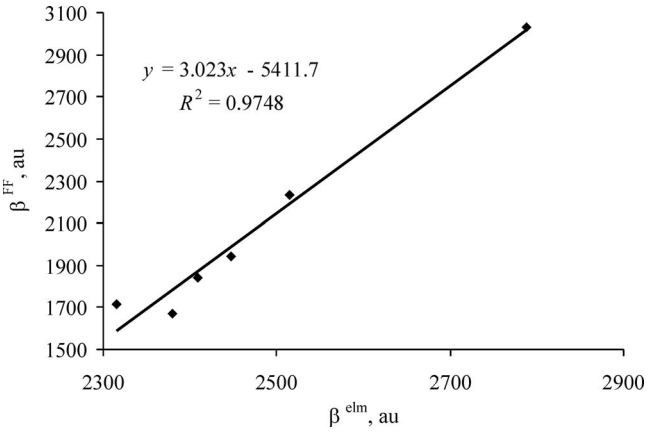

FIG. 2. Correlation between hyperpolarizabilities of *p*NA dimers obtained by finite field method (β^{FF}) and electrostatic model (β^{elm}).

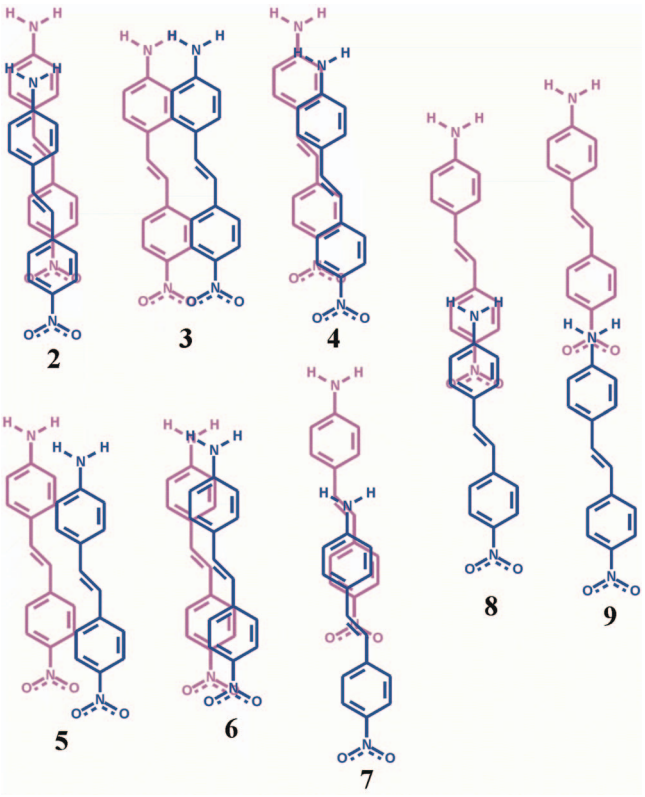

SCHEME 4. Types of ANS dimers studied.

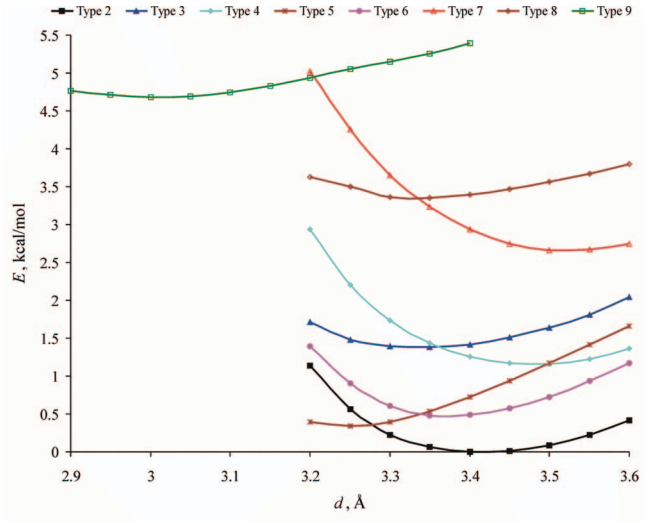

FIG. 3. Dependence of the interaction energy (E, kcal/mol) on the interplanar separation (d, Å) for different dimer types.

difference between Types 3 and 6 is rather small. Calculated values of β^{elm} for Types 2–6 appear to be somewhat smaller than the sum of two monomer values; for Type 7 it is nearly twice of monomeric β while the accurate dimer hyperpolarizability (Table I) shows slight increase relative to the monomeric sum. In general, the proposed approach overestimates hyperpolarizability by 20%–50% for those cases when molecular aggregation leads to a decrease of β relative to additive sum and underestimates the accurate hyperpolarizability (by 10%) in other cases. Apparently, these inaccuracies are the result of the uniform field used to approximate intermolecular interactions of a more complex shape. Another reason is a neglect of the effect of mutual polarization of the molecules in dimer upon perturbation by the electric field. Nevertheless, nearly linear dependence of β^{FF} vs β^{elm} is obtained which can improve a predictive ability of the electrostatic model.

To validate an efficiency of our computational approaches we considered dimers formed by the molecules with extended π-conjugated bridge, specifically NH_2/NO_2-stilbene (ANS). Here we considered several types of ANS dimers depicted in Scheme 4, following the same principles discussed earlier for *p*NA. Both excitonic and electrostatic models approximate intermolecular interactions by point dipoles, which is not very accurate when intermolecular separation is comparable with the size of the molecules. Therefore, one can expect reduced accuracy of these models when hyperpolarizabilities of ANS dimers are calculated.[137]

In case of ANS dimers, Types 2–6 are similar to those of *p*NA, Types 7 and 8 are new and cannot be observed for *p*NA while Type 9 resembles Type 7 of *p*NA. Optimal interplanar separation was determined in the same way described above for *p*NA. Dependence of the energy upon interplanar separation is presented in Figure 3. The results obtained for the most energetically favorable dimers of each type are listed in Table III.

When two molecules in a dimer do not slide significantly with respect to each other (as is the case for Types 2–7), the electrostatic and exciton models predict the same trends as more rigorous finite field method, similar to the case of *p*NA above. Exciton model predicts increase of β in the series of Type6 < Type3 < Type5 < Type4 < Type2 < Type7 in agreement with FF theory. However, exciton model predicts enhancement of β for Types 2 and 7 in contrast to FF results which show that for Types 2–7 hyperpolarizability of dimer is decreased relative to additive sum of monomers. At the same time results of electrostatic model show lowering of β for dimers of Types 2–7 relative to additive monomeric sum; however, the value of β^{elm} of Type 6 is not predicted to be the smallest one. One should note that exactly the same situation was observed for *p*NA dimer of the Type 6. ANS molecules in dimers of Types 8 and 9 are significantly shifted relative to each other and, as expected, this makes the results of both exciton and electrostatic models less accurate. This is clearly shown in the plot of β^{FF} vs β^{elm} (Figure 4). The results for Types 2–7 demostrate nearly linear correlation between β^{FF} and β^{elm} (correlation coefficient (R) is somewhat lower than that for *p*NA) while Types 8 and 9 have to be separated into another group.

Another observation one can make from Table III is the absence of correlation between intermolecular interaction energy of a dimer and hyperpolarizability, in line with *p*NA results.

One can conclude that both exciton and electrostatic models provide qualitative explanation of trends in hyperpolarizability variations upon different ways of aggregation which allows one to make the following conclusions: (a) hyperpolarizability of an aggregate depends on the electric filed induced by molecules on each other (in other words, on the

TABLE III. Energies, hyperpolarizabilities, dipole moments, and parameters of Eq. (6) obtained by finite field and electrostatic approximations, for different Types of ANS dimers.

	2 monomers[a]	Type2	Type3	Type4	Type5	Type6	Type7	Type8	Type9
Energy E (kcal/mol)	7.67	0.00	1.38	1.16	0.34	0.48	2.66	3.35	4.69
Interplanar separation d (Å)	∞	3.40	3.35	3.50	3.25	3.35	3.50	3.35	3.00
Intermolecular distance R (Å)	∞	4.398	4.128	4.252	4.269	3.632	7.043	9.996	12.622
Angle α (deg)	...	50.8	87.4	61.9	73.4	79.9	29.8	19.6	13.8
$\frac{1-3\cos^2\theta}{R^3}$ (Å^{-3})	0	-2.3×10^{-3}	14.1×10^{-3}	4.3×10^{-3}	9.7×10^{-3}	19.0×10^{-3}	-3.6×10^{-3}	-1.7×10^{-3}	-0.9×10^{-3}
β^{elm}(1st mol[b]) (au)	...	11 042	8004	10 239	10 477	9506	10 966	5997	7763
β^{elm}(2nd mol) (au)	...	9341	8059	8412	7693	7575	13 047	13 533	13 492
β^{elm}(total) (au)	24 974	20 383	16 063	18 651	18 170	17 081	24 013	19 530	21 255
β^{FF} (au)	24 528	16 902	15 280	15 723	15 354	14 840	20 990	28 637	31 241
Dipole (μ) (D)	19.38	18.33	18.10	18.23	18.09	18.18	18.64	19.02	19.82

[a]Twice the values of energy, hyperpolarizability, and dipole moment of isolated monomer of ANS are given for a comparison.
[b]The first molecule corresponds to the bottom one shown in light pink color in Scheme 4.

relative orientation of the molecular dipole moments) rather than intermolecular interaction energy and (b) linear correlation between βFF and βelm is observed for pNA dimers and dimers of ANS in which two molecules do not slide significantly relative to each other.

To avoid above mentioned limitations of presented electrostatic model we have calculated hyperpolarizabilities of the *p*NA and ANS dimers in which the second molecule in a dimer is replaced by two point charges located at the opposite ends of a molecule: positive charge is located at the donor end while negative is at acceptor end. Value of charges is taken so that to reproduce the dipole moment of isolated *p*NA and ANS molecules. Hyperpolarizabilities of both molecules constituting a dimer can be separately calculated by placing of charges in corresponding positions (see Figure 6S in the supplementary material[132]). Such an approach is also based on electrostatic laws; however, it is free of limitation of the point dipole approximation because charges induce nonuniform field on a molecule. Nevertheless, the effect of mutual polarization of molecules in a dimer upon perturbation by the electric field cannot be taken into account. As expected, the results obtained by this charge model (CM) are in much better agreement with finite field calculations and demonstrate linear correlation with β^{FF} with higher correlation coefficient and a slope close to 1 for all dimer Types considered (Figure 5 and Tables 4S and 5S in the supplementary material[132]).

At the same time proposed charge model is much less general than proposed electrostatic model, because in each case, separate calculation of the molecular hyperpolarizability with appropriate orientation of the point charges is necessary

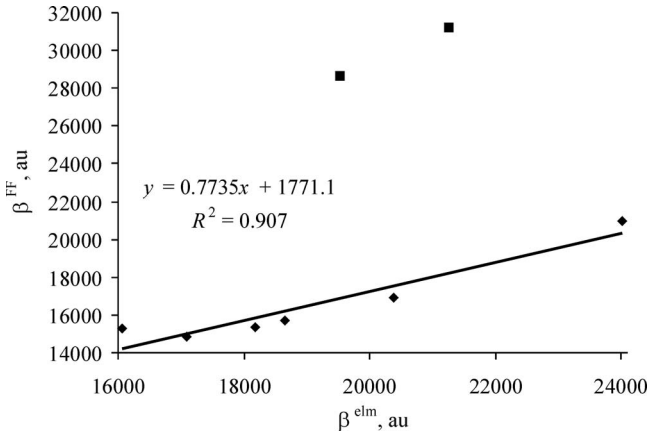

FIG. 4. Correlation between hyperpolarizabilities of ANS dimers obtained by finite field method (β^{FF}) and electrostatic model (β^{elm}).

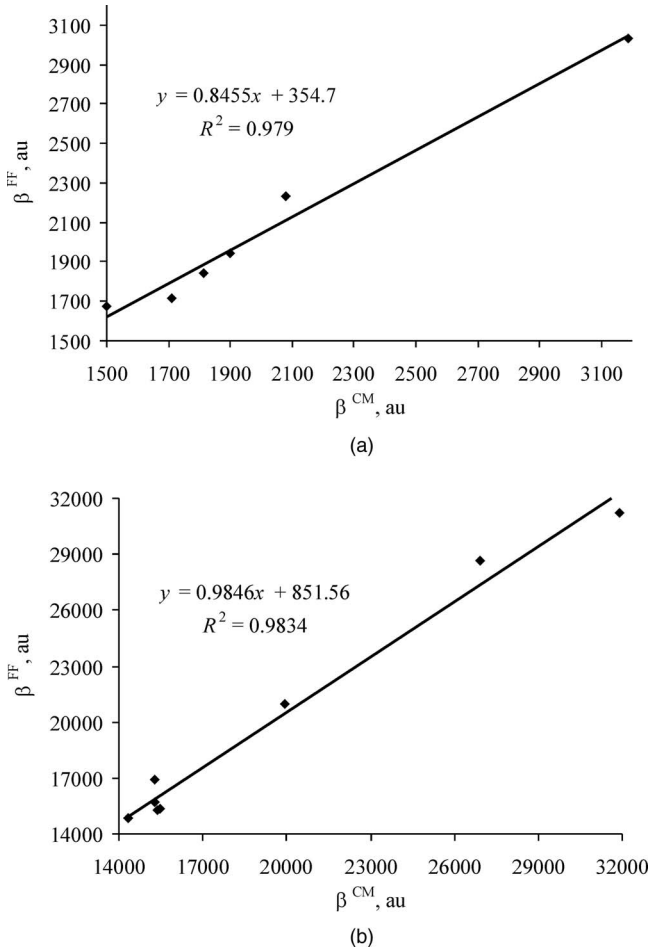

FIG. 5. Correlation between hyperpolarizabilities of *p*NA dimers (a) and ANS dimers (b) obtained by finite field method (β^{FF}) and charge model (β^{CM}).

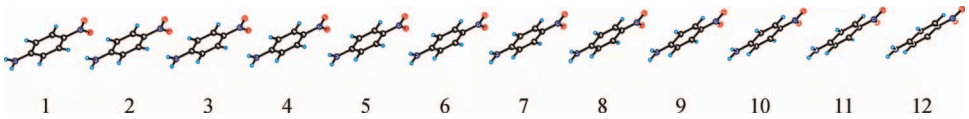

FIG. 6. *p*NA stacking aggregate of Type 7, showing the molecular numbering scheme.

to carry out, while in the electrostatic model one needs to substitute the charge of the nitro group into the linear regression β^{elm} vs q_{NO2}. Also, use of linear correction of β^{FF} vs β^{elm} (as will also be shown in Sec. III B) can significantly improve predictive ability of the electrostatic model.

B. Larger stacking aggregates

Cooperative effects are critically important in crystals, films, and one-dimensional (1D) aggregates, which contain a very large number of molecules. In 1D stack, intermolecular interactions with only two nearest neighbors produce the most significant effect, hence at least three molecules must be included into the model system selected for the calculation. Further addition of molecules to the stack would affect the central molecule both directly through space, and indirectly by polarizing the second and third molecule. Apparently, the effect of each additional molecule will saturate upon the cluster growth. Ideally, one should be able to extrapolate the asymptotic limit of infinite stack based on the data for a few small clusters. Therefore we need to determine how many molecules are sufficient to describe intermolecular effects with reasonable accuracy. There is also related question of how this sufficient cluster size depends on the type of interaction.

To address these questions we have considered stacks of the growing size (up to 12 molecules) for several different types of *p*NA (Types 2, 3, and 7). Types 2 and 7 correspond to the most energetically favorable, yet geometrically different intermolecular interactions. In contrast, Type 3 represents the most unfavorable way of stacking aggregation and demonstrates the most pronounced negative deviation from additivity (negative cooperative hyperpolarizability). We have also calculated hyperpolarizability of Type 2 stack built up of ANS molecules. At the end of this section, stacking aggregates which are observed in real crystal structures of two well known NLO compounds MNMA, NPAN are described. Numbering of molecules in a stack is shown in Figure 6 for Type 7 *p*NA stack as an example. The results of calculation of *p*NA and ANS stacks are presented in Tables IV and V and in Figures 7–9 (see also Tables 6S–8S and Figure 7S in the supplementary material[132]).

TABLE IV. Hyperpolarizabilities of *p*NA stacking aggregate of Type 7 obtained by FF and electrostatic methods.

	Number of molecules in a stack											
β_n	1	2	3	4	5	6	7	8	9	10	11	12
	Hyperpolarizabilities obtained by electrostatic model (M05-2X/6-31+G*)											
β_1	1404	1309	1330	1341	1346	1349	1350	1351	1352	1352	1353	1353
β_2		1479	1383	1408	1420	1426	1428	1430	1431	1432	1432	1432
β_3			1514	1417	1442	1455	1460	1463	1465	1466	1467	1467
β_4				1527	1430	1456	1468	1474	1477	1479	1480	1480
β_5					1534	1436	1461	1474	1480	1483	1485	1486
β_6						1537	1439	1464	1477	1483	1486	1488
β_7							1538	1440	1466	1479	1485	1488
β_8								1540	1442	1467	1480	1486
β_9									1540	1442	1468	1481
β_{10}										1541	1443	1468
β_{11}											1541	1443
β_{12}												1542
β_{tot}	1404	2788	4227	5693	7172	8658	10 145	11 637	13 130	14 624	16 120	17 616
$\beta_n - \beta_{n-1}$		1384	1439	1466	1479	1487	1486	1492	1493	1495	1495	1496
$\frac{\beta_n - \beta_{n-1}}{\beta_1}$		0.985	1.025	1.044	1.053	1.059	1.058	1.062	1.063	1.065	1.065	1.065
	Hyperpolarizabilities obtained by FF method (M05-2X/6-31+G*)											
β_{tot}	1404	3031	5136	7534	10 093	12 738	15 435	18 165	20 912	23 680	26 451	29 227
$\beta_n - \beta_{n-1}$		1627	2105	2398	2559	2645	2697	2730	2747	2768	2771	2776
$\frac{\beta_n - \beta_{n-1}}{\beta_1}$		1.159	1.499	1.708	1.823	1.884	1.921	1.944	1.957	1.972	1.974	1.977
	Hyperpolarizabilities obtained by FF method (M05-2X/6-31G)											
β_{tot}	1373	2966	4954	7236	9585	12 001	14 443	16 915	19 396	21 881	24 383	26 894
$\beta_n - \beta_{n-1}$		1593	1988	2282	2349	2416	2442	2472	2481	2485	2502	2511
$\frac{\beta_n - \beta_{n-1}}{\beta_1}$		1.160	1.448	1.662	1.711	1.760	1.779	1.800	1.807	1.810	1.822	1.829

TABLE V. Hyperpolarizabilities of stacks of *p*NA of Types 2 and 3 and ANS of Type 2 obtained by finite field method at M05-2X/6-31G theory level.

	Number of molecules in a stack											
	1	2	3	4	5	6	7	8	9	10	11	12
						*p*NA Type 2						
β_{tot}	1373	2358	3437	4595	5797	7034	8282	9541	10 804	12 085	13 371	14 658
$\beta_n - \beta_{n-1}$		985	1079	1158	1202	1237	1248	1259	1263	1281	1286	1287
$\frac{\beta_n - \beta_{n-1}}{\beta_1}$		0.717	0.786	0.843	0.875	0.901	0.909	0.917	0.920	0.933	0.937	0.937
						*p*NA Type 3						
β_{tot}	1373	1848	2319	2788	3255	3720	4183	4645	5108	5569	6029	6489
$\beta_n - \beta_{n-1}$		475	471	469	467	465	463	462	463	461	460	460
$\frac{\beta_n - \beta_{n-1}}{\beta_1}$		0.346	0.343	0.342	0.340	0.339	0.337	0.336	0.337	0.336	0.335	0.335
						ANS Type 2						
β_{tot}	12 371	17 426	22 685	28 149	33 792	39 531	45 352	51 258	57 219	63 205	69 220	75 233
$\beta_n - \beta_{n-1}$		5055	5259	5464	5643	5739	5821	5906	5961	5986	6015	6013
$\frac{\beta_n - \beta_{n-1}}{\beta_1}$		0.409	0.425	0.442	0.456	0.464	0.471	0.477	0.482	0.484	0.486	0.486

We start the discussion from the stack of Type 7, which is the most energetically favorable. As one can see from Table IV and Figure 7, this way of aggregation leads to enhancement of hyperpolarizability, according to the results of finite field calculations. Addition of the third molecule to the dimer results in more pronounced effect on β than that found upon dimerization. Upon further increase of the stack size the nonlinear growth of β slows down. The most significant changes are observed for two to six monomer stacks. Changes upon the stack growth to 7 and 8 molecules are smaller but not negligible, while further size increase produces insignificant effect. Estimation of $\Delta\beta_\infty/\beta_1$ is obtained using stacks of different sizes (6, 8, 10, and 12 molecules) and presented below in Table VII which summarizes different ways to extrapolate to the asymptotic limit of β.

The results of FF calculation on Type 7 stacks can be explained within electrostatic approach, which estimates individual contributions to the total value of hyperpolarizability. The electrostatic approach correctly describes the trends in hyperpolarizability in the stacks of growing size as well as saturation limit; however, it underestimates the effect of the molecular aggregation. One can see that formation of a trimer leads to a larger deviation of β from the additive assumption, than formation of a dimer. The addition of the next molecule to trimer, tetramer, etc. has more pronounced effect on the central molecules of a stack and not on the terminal molecules. The most significant effect of intermolecular interactions is produced by two nearest neighbors on each side. When the stack is formed by 8 molecules, no further size increase leads to any significant change in hyperpolarizabilities. Calculated molecular contributions to the total hyperpolarizability show that extrapolation to the asymptotic hyperpolarizability of infinite cluster using $\beta_n - \beta_{n-1}$ difference is more reliable than by β_n/n ratio because the former cancels the effect of terminal molecules, instead of spreading it. What is the most important, is the observed correlation β^{FF} vs β^{elm} that is plotted in Figure 8. Dependence is exactly linear ($R = 1$). This finding allows to significantly reduce time of calculation. It is now enough to do explicit calculations with 2 and 3 molecules in order to obtain the coefficient in the linear equation $\beta^{FF} = k \times \beta^{elm} + b$. With this equation hyperpolarizability of a stack of any size can be immediately predicted at nearly quantitative level of accuracy.

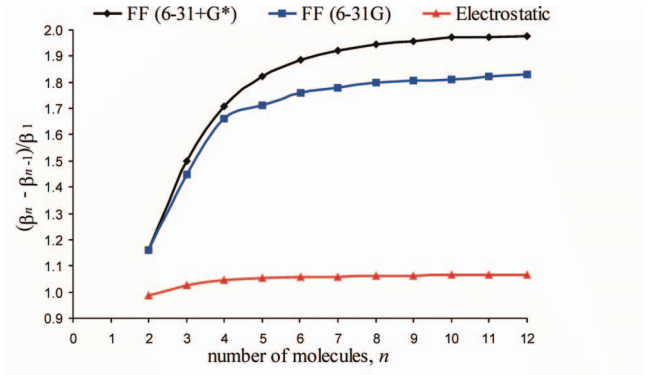

FIG. 7. The relative hyperpolarizability per molecule as a function of the number of molecules (n) in *p*NA stack of Type 7 obtained by FF and electrostatic methods.

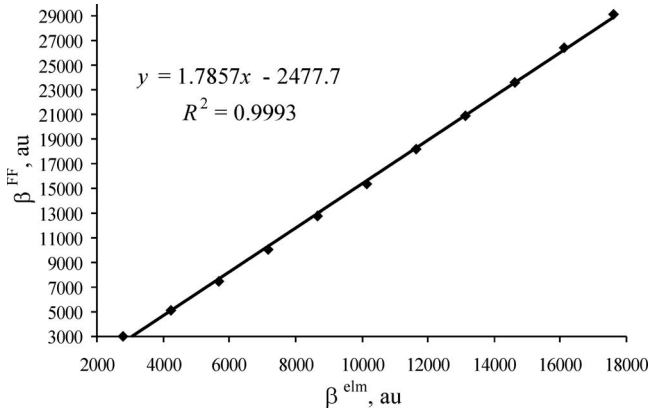

FIG. 8. Correlation between hyperpolarizabilities of Type 7 *p*NA stacks (n = 2–12) obtained by finite field method (β^{FF}) and electrostatic model (β^{elm}).

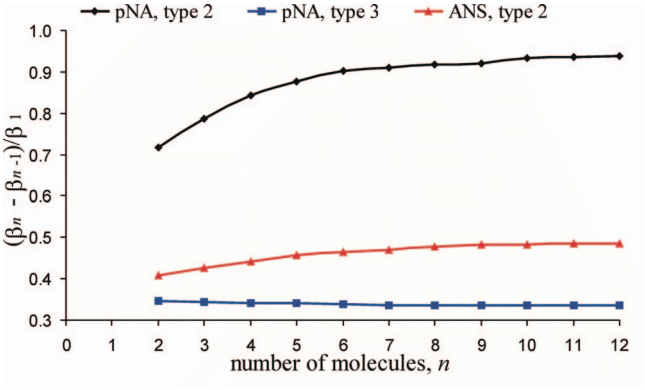

FIG. 9. Dependence of relative hyperpolarizability per molecule on number of molecules (n) in pNA stacks of Types 2 and 3 and ANS stack of Type 2.

In Table VII we also presented extrapolated to infinity βs obtained with $1/2(\beta_n - \beta_{n-2})$ formula. According to the data obtained with the electrostatic model, this formula seems to be also adequate. For Type 7 we also studied an effect of reduction of the basis set from 6-31+G* to 6-31G (see bottom of Table IV). The difference between $(\beta_n - \beta_{n-1})/\beta_1$ ratios do not exceed 15% which is somewhat higher than it was observed in our previous study on mNA stacking aggregate[121] but it is still smaller than expected uncertainty of theoretical prediction. Based on these results all the remaining stacking aggregates were calculated at M05-2X/6-31G level of theory to avoid convergence problems.

The results obtained for pNA stacks of Types 2 and 3 (Table V, Figure 9, and Tables 3S and 4S and Figure 7S in the supplementary material[132]) show some similarities as well as some differences relative to Type 7.

The differences with Type 7 arise from two opposite effects which exist for aggregates with negative deviation of β from additive sum and are not observed for molecular aggregation which leads to an enhancement of hyperpolarizability. On one hand, addition of the third molecule to a dimer decreases β of its closest neighbor (2nd molecule). On the other hand, this results in a decrease of the dipole moment of this second molecule thereby leading to a decrease of the dipole-dipole interaction between second and first molecules, which in turn weakens their effect on each other (decreases negative deviation from additive model). In the case of Type 3, these opposite effects cancel each other which leads to nearly constant value of $(\beta_n - \beta_{n-1})/\beta_1$. One can also see this from consideration of the separate molecular contributions (Table 7S in the supplementary material[132]). The second molecule in the dimer becomes the central molecule in the trimer. Decrease of its hyperpolarizability is much smaller than that observed upon the dimer formation and negligible decrease of β is found for the first (terminal) molecule which is equal to β of the third molecule (see Figure 6 for molecular numbering in a stack). Extrapolation of molecular hyperpolarizability to the infinite stack is given in Table VII and is discussed below.

For the dimers of Type 2 negative cooperativity of hyperpolarizability is weaker (negative deviation from additive sum is smaller). As one can see from Table V, Figure 9, and Table 6S in the supplementary material[132] with each additional molecule the deviation of actual hyperpolarizability from additive estimate decreases, and the $(\beta_n - \beta_{n-1})/\beta_1$ value increases. Similar to Type 7, the most pronounced changes in hyperpolarizability are observed for the stacks of six molecules or less. In a sharp contrast with the trends observed for Type 7, those changes are much smaller in comparison to changes in β upon the dimer formation.

The results on Type 2 stacking aggregation of ANS molecules show the trends in hyperpolarizability changes (Table V, Figure 9, and Table 8S in the supplementary material[132]) similar to the ones observed for Type 2 pNA stacks. Due to the higher dipole moment of ANS, one can observe stronger intermolecular effect on β is revealed already in the dimers. Each additional molecule brings about smaller increase of relative hyperpolarizability ($(\beta_n - \beta_{n-1})/\beta_1$) in comparison to Type 2 pNA stacks. The results of individual molecular contributions to total hyperpolarizability (Tables 6S–8S in the supplementary material[132]) obtained with electrostatic model for Type 2 stacks clearly show that the most significant effect of intermolecular interaction is observed for the central molecules of a stack while hyperpolarizability of terminal molecules does not change much.

Again as in the case of Type 7 pNA stack, we have plotted β^{FF} vs β^{elm} for above considered stacks (Figure 7S in the supplementary material[132]) which demonstrate exactly linear correlation.

C. Stacks from the crystal structures of NPAN and MNMA

For the calculation of NLO properties of NPAN and MNMA aggregates we used X-ray geometries in which C–H and N–H bonds were renormalized to the standard neutron diffraction values of 1.09 Å for C–H and 1.01 Å for N–H bond lengths. In the crystal structures of both compounds $\pi\ldots\pi$ stacking interactions are observed (Figure 10).

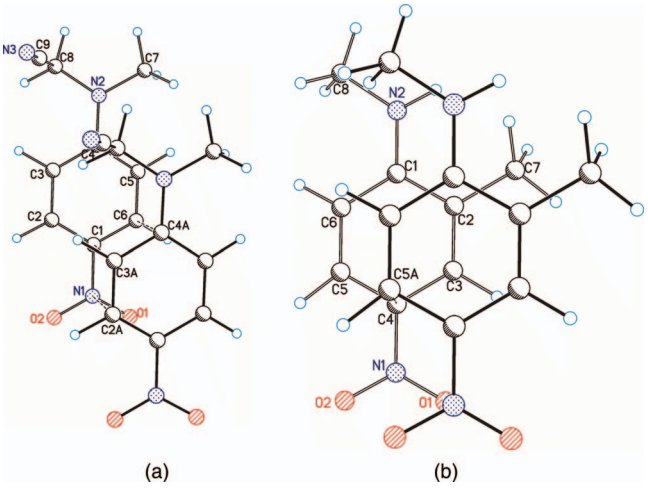

FIG. 10. Structure of stacking dimers of NPAN (left) and MNMA (right) taken from X-ray data. In all dimers molecules in stacks are related by a translation along c axis. The shortest intermolecular contacts are shown by dashed lines. For NPAN: interplanar separation is 3.488 Å, the shortest contacts are N1…C2 (3.465 Å), C1…C3 (3.505 Å), C6…C4 (3.508 Å). For MNMA: interplanar separation is 3.491 Å, the shortest contact is C4…C5 (3.499 Å).

TABLE VI. Hyperpolarizabilities of stacks of NPAN and MNMA obtained by finite field method at M05-2X/6-31G theory level.

	Number of molecules in a stack											
	1	2	3	4	5	6	7	8	9	10	11	12
						NPAN						
β_{tot}	1901	2639	3442	4277	5114	5977	6844	7713	8582	9457	10 330	11 205
$\beta_n - \beta_{n-1}$		738	803	835	837	863	867	869	869	875	873	875
$\frac{\beta_n - \beta_{n-1}}{\beta_1}$		0.388	0.422	0.439	0.440	0.454	0.456	0.457	0.457	0.460	0.459	0.460
						MNMA						
β_{tot}	1675	2099	2546	3001	3463	3932	4406	4877	5349	5818	6297	6770
$\beta_n - \beta_{n-1}$		424	447	455	462	469	474	471	472	469	479	473
$\frac{\beta_n - \beta_{n-1}}{\beta_1}$		0.253	0.267	0.272	0.276	0.280	0.283	0.281	0.282	0.280	0.286	0.282

Stack of NPAN closely resembles that of Type 4 of *p*NA, while stacking aggregation of MNMA molecules is similar to Type 6 of *p*NA. The results of calculation are shown in Table VI. MNMA stacks demonstrate more pronounced lowering of β than NPAN ones, in agreement with the results of similar *p*NA stacks (Type 6 shows larger negative deviation than Type 4). Again, in the case of NPAN, more significant changes of β are found for stacks built up of one to six molecules while three molecules of MNMA in the stack appear to be sufficient to reproduce intermolecular effect on β.

We estimated hyperpolarizability of infinite stacks using expression[144]

$$\Delta\beta_n/\beta_1 = \alpha - b \cdot e^{-cn}$$

(where n is a number of molecules in a stack) and summarized the results in Table VII. In fact these results show a role of a cooperative effect and agree with conclusions made earlier in this section. The value of $\Delta\beta_n$ was obtained in two different methods according to general expression

$$\Delta\beta_n = x \cdot (\beta_n - \beta_{n-m}).$$

In the first (more common) method we used $x = 1$ and $m = 1$ while in the other method we used $x = 1/2$, $m = 2$, and even n. The results obtained with the first method clearly show that stack of six molecules appears to be sufficient for reliable estimation of $\Delta\beta_\infty/\beta_1$. This value does not deviate by more than few percent when obtained from 12-molecules stack, while no difference is observed for infinite hyperpolarizability estimated from 8-, 10-, and 12-molecule stacks. Comparison of $\Delta\beta_\infty/\beta_1$ and $\Delta\beta_n/\beta_1$ from Tables IV–VI show that for $n = 8$ one can use $\Delta\beta_n/\beta_1$ ratio without fitting procedure to estimate $\Delta\beta_\infty/\beta_1$ within 1%–3%. This error is the highest for Type 7 *p*NA stack for which intermolecular effects lead to the enhancement of β. Even ratio of $\Delta\beta_{n=6}/\beta_1$ (again without fitting procedure) can be used for stacks which are characterized by a significant negative deviation from oriented gas model. For such stacks, truncation of the stack size is the less significant. Moreover in *p*NA stacks of Type 3, the dimers are already sufficient to describe intermolecular effects. The results of estimation of $\Delta\beta_n$ using the second method demonstrate general agreement with the data above. This method can be particularly helpful for molecular stacks or chains in which two closest molecules are not related by a translation symmetry that leads to cancellation of some tensor components and complicates comparison with additive model. In such aggregates the 1D repeating unit consists of the two molecules, and one can use dimers rather than monomers to build the aggregates.

While discussing the effect of the intermolecular interactions on hyperpolarizability, one may consider an additional aspect. It might so happen that components of molecular hyperpolarizability tensor, which are strongly affected by intermolecular interactions, are cancelled in the crystal due to its symmetry. In this case, the effect of the molecular

TABLE VII. Molecular hyperpolarizabilities calculated at M05-2X/6-31G approximation and estimated for stacking aggregate of infinite size.

	Stack size						
	$\Delta\beta_n = \beta_n - \beta_{n-1}$ $(n > 1)$				$\Delta\beta_n = \beta_n - \beta_{n-2}$, n – even; n > 2		
Stacking aggregate	6	8	10	12	8	10	12
*p*NA, Type 7	1.81(4)	1.81(2)	1.812(9)	1.818(7)	1.81	1.817(6)	1.825(6)
*p*NA, Type 7[a]	1.979(12)	1.974(4)	1.977(2)	1.979(2)	1.97	1.977(3)	1.979(2)
*p*NA, Type 3	0.335(3)	0.332(3)	0.335(2)	0.334(2)	0.32	0.335(2)	0.334(2)
*p*NA, Type 2	0.96(2)	0.937(6)	0.937(4)	0.939(3)	0.93	0.932(4)	0.938(4)
ANS, Type 2	0.52(3)	0.501(7)	0.498(3)	0.494(2)	0.49	0.493(2)	0.492(2)
NPAN	0.455(7)	0.460(4)	0.459(2)	0.460(2)	0.47	0.461(4)	0.461(2)
MNMA	0.282(3)	0.284(2)	0.281(2)	0.283(2)	0.29	0.281(4)	0.284(4)

[a]Results for M05-2X/6-31+G*.

TABLE VIII. Crystal nonlinear optical susceptibility (in pm/V) of NPAN and MNMA: theory vs. experiment.

	NPAN			MNMA		
	d_{xxz}	d_{yyz}	d_{zzz}	d_{xxz}	d_{yyz}	d_{zzz}
Experiment[a]	...	48	24	13	...	2.6
Oriented gas model	0.3	11.4	2.6	5.2	0.3	0.8
Supermolecule approach	0.1	6.2	2.9	2.1	0.1	0.9

[a]Experimental data for NPAN measured at 1340 nm[131]; for MNMA measured at 1340 nm.[130]

environment on nonlinear susceptibility would not appear significant in comparison with oriented gas model. This however does not mean that intermolecular effects are absent in the crystal structure. Completely reverse case is also possible as well as intermediate cases, depending on the relative orientation of molecules in the crystal unit cell. The nonlinear susceptibility tensor components were calculated by Eq. (4). According to *mm*2 class of symmetry, only three nonvanishing components of d_{ijk} tensor can exist in the crystal structure of both NPAN and MNMA. For both compounds, only two components of d_{ijk} were measured. Comparison of experimental and theoretical values is presented in Table VIII.

According to our results, obtained with both oriented gas model (additive estimate) and supermolecule approach (taking into account stacking interactions only), the values of d_{xxz} for NPAN and d_{yyz} for MNMA nearly cancel. It can be the reason why they were not measured. At the same time in the case of NPAN, additive model does not explain the ratio of d_{zzz}/d_{yyz}, while an account for an effect of stacking interactions significantly improve an agreement with experiment $(d_{yyz}/d_{zzz})_{EXP} = 2.0$; $(d_{yyz}/d_{zzz})_{CALC} = 2.1$. To the contrary, oriented gas model works quite well for MNMA while an account for stacking interactions leads to larger deviations. This result is however expected and can be easily explained by consideration of the crystal packing of the NPAN and MNMA. In addition to van der Waals and stacking interactions (observed for NPAN), the crystal structure of MNMA is also stabilized by head-to-tail H-bonding that should increase hyperpolarizability. This follows from literature data discussed in the Introduction and is explained by the Frenkel exciton model. Therefore in the case of MNMA, lowering of β due to stacking interactions compensates its enhancement by H-bonding. Neglect of H-bonding effect, van der Waals interactions as well as frequency dependence are probably responsible for the differences between the calculated and experimental absolute values of d_{ijk} tensor.

TABLE IX. Frequency-dependent hyperpolarizabilities (at $\lambda = 1340$ nm) of stacks of NPAN obtained at M05-2X/6-31G theory level.

	Number of molecules in a stack					
	1	2	3	4	5	6
β_{tot}	2525	3451	4486	5554	6641	7739
$\beta_n - \beta_{n-1}$		926	1035	1068	1087	1098
$\frac{\beta_n - \beta_{n-1}}{\beta_1}$		0.367	0.410	0.423	0.430	0.435

While detailed study on H-bonding effects on hyperpolarizability is not the subject of the present study, here we estimated the effect of frequency dependence in case of NPAN. We have restricted calculation by the stack size equal to six molecules (according to conclusions given above). The results are listed in Table IX.

Comparison of Tables VI and IX shows that frequency-dependent hyperpolarizability of the monomer is higher than static value by 33%; however, relative decrease upon stack formation is nearly the same (0.436(3) for frequency-dependent calculation and 0.455(7) for static one). Estimated dynamic nonlinear optical susceptibility tensor components in crystal are closer to experimental ones as expected ($d_{xxz} = 0.1$; $d_{yyz} = 7.7$; $d_{zzz} = 3.4$ pm/V).

IV. CONCLUSIONS

In this paper we investigated the possibility of theoretical prediction of optical nonlinearities in molecular crystals. Our objective was to find sufficiently accurate and relatively simple way to account for effects of intermolecular interaction which can lead to significant changes of properties relative to those obtained as simple additive model (tensorial sum of properties of the isolated molecules). Our study was focused on π-π stacking interaction and addressed several inportant aspects: (i) type of the interaction, defined by relative orientation of the molecules; (ii) physical reasons affecting the hyperpolarizability of aggregate; (iii) means of interpreting the results; and (iv) minimal size of the aggregate necessary to predict the asymptotical limit (cooperative effects).

We considered several modes of stacking between D/A-substituted benzene and stilbene molecules, that include different overlap of molecular π-systems. The results obtained lead us to the following conclusion: hyperpolarizability of the molecular aggregate depends on mutual orientation of the dipole moments of the interacting molecules (electrostatic energy) rather than on the total interaction energy. The Frenkel exciton model, which is based on point dipole-dipole scheme, can be successfully utilized for qualitative explanation of hyperpolarizability variation upon different ways of molecular orientation in a stack. If mutual orientation of two molecules corresponds to repulsive interaction of their dipoles, then hyperpolarizability of an aggregate is negatively cooperative (smaller than additive sum). The stronger this dipole-dipole repulsion is, the more pronounced is the negative deviation (decrease) of β from the additive model. Attractive dipole-dipole orientation leads to an enhancement of β. Again, the stronger is the attraction, the larger is the enhancement.

In order to interpret the variation of β among the different Types of molecular stacking, we proposed a simple electrostatic model which accounts for the ground state polarization of the molecule by its neighbors. To quantify an effect of polarization we used the charge on the acceptor group (q_{NO2}). Dependence of hyperpolarizability on polarization and, as a consequence, on the charge q_{NO2} (β vs. q_{NO2}) can be easily calculated and appears to be linear. The correlation between β and q_{NO2} allows one to estimate the individual β values of

each molecule in the aggregate. This electrostatic model explains hyperpolarizability changes at qualitative level for relatively small conjugated molecules such as pNA. Although one may expect the inaccuracy of this model to increase with the size of individual molecule, the model works well for NH2/NO2-substituted stilbene. The proposed electrostatic model has two significant advantages. First, it allows to estimate individual contributions of molecular hyperpolarizabilities into the total β of an aggregate. This is especially helpful to study the effect of intermolecular interactions in stacking aggregates of growing size. Second, it is the observed linear correlation β^{FF} vs β^{elm} in considered stacks. Correlation coefficient of the linear regression is found to be near unity that allows to obtain $\beta^{FF} = k \times \beta^{elm} + b$ equation by a consideration of relatively small stack (2 and 3 molecules) and predict the value of β^{FF} for a stack of arbitrary size that significantly decreases computational cost.

The analysis of individual molecular contributions reveals that the most significant effect on the molecular hyperpolarizability is found for smaller stacks (two to six molecules). The β values of central molecules are affected to a greater extent than terminal molecules which have a neighbor on one side only. The cancelation of contributions from the terminal molecules justifies the choice of $\beta_n - \beta_{n-1}$ rather than β_n/n expression for an estimation of molecular hyperpolarizability for an infinite stack.

Stacking interaction typically lowers the β relative to additive approximation. Addition of each molecule to the growing stack generates two opposite effects. The first one is a decrease of dipole moments of the molecules in a stack and respective decrease of their βs. At the same time, decrease of molecular dipole moments is decreasing intermolecular effect, which in turn leads to increase of β. The relative importance of these two opposite trends depends on the strength of dipole-dipole interactions which can be quantified by a degree of lowering of β upon a dimer formation. In the case of relatively weak dipole-dipole interactions, lowering effect is smaller than the effect of weakening of dipole-dipole interactions between molecules which results in the growth of hyperpolarizability (in the case of Type 2 *p*NA stack this leads to nearly insignificant effect of stacking interaction on β ~6%). The stronger this dipole-dipole interaction is, the closer the contributions of two opposite effects are. This means that effect of molecular aggregation on β can be correctly predicted by a consideration of dimers.

The results obtained here show that in general the effects of intermolecular surrounding on hyperpolarizability are not negligible and must be considered. They depend on the orientation of the molecules in the unit cell and on the symmetry of the crystal. In some cases it can lead to a cancellation (or partial cancellation) of components of hyperpolarizability tensor which are mostly affected by an intermolecular interactions. This however does not mean that surroundings of a molecule have no effect on its hyperpolarizability in general. We suggest that for a preliminary estimate of the intermolecular effect one has to consider the closest neighbors. For the case of stacking columns this means a trimer. However, for an accurate description of stacking interactions, stacks of six or eight molecules need to be calculated.

ACKNOWLEDGMENTS

This work was supported in part by the National Science Foundation (CHE-0832622) and Russian Foundation for Basic Research (Grant 13-03-01041). The authors are grateful to the anonymous reviewer for their valuable suggestions. This research used resources of the University of Central Florida Stokes Advanced Research Computing Center, and National Energy Research Scientific Computing Center, which is supported by the Office of Science of the U.S. Department of Energy under Contract No. DE-AC02-05CH11231.

[1](a) L. R. Dalton, W. H. Steier, B. H. Robinson, C. Zhang, A. Ren, S. Garner, A. T. Chen, T. Londergan, L. Irwin, B. Carlson, L. Fifield, G. Phelan, C. Kincaid, J. Amend, and A. Jen, J. Mater. Chem. **9**, 1905 (1999); (b) Y. Q. Shi, C. Zhang, H. Zhang, J. H. Bechtel, L. R. Dalton, B. H. Robinson, and W. H. Steier, Science **288**, 119 (2000); (c) L. R. Dalton, P. A. Sullivan, and D. H. Bale, Chem. Rev. **110**, 25 (2010).
[2]L. González-Urbina, K. Baert, B. Kolaric, J. Pérez-Moreno, and K. Clays, Chem. Rev. **112**, 2268 (2012).
[3]*Handbook of Advanced Electronic and Photonic Materials and Devices. Nonlinear Optical Materials*, edited by H. S. Nalwa (Academic Press, San Diego, 2000), Vol. 9.
[4]S. R. Marder, Chem. Commun. 131 (2006).
[5]*Nonlinear Optical Properties of Organic Molecules and Crystals*, edited by D. S. Chemla and J. Zyss (Academic Press, Orlando, 1987).
[6]J. Zyss and I. Ledoux, Chem. Rev. **94**, 77 (1994).
[7]F. Wurthner, R. Wortmann, and K. Meerholz, Chem. Phys. Chem. **3**, 17 (2002).
[8]K. Y. Suponitsky, T. V. Timofeeva, and M. Y. Antipin, Usp. Khim. **75**, 515 (2006).
[9]B. Champagne, Chem. Modell. **6**, 17 (2009).
[10]P. Salek, O. Vahtras, T. Helgaker, and H. Agren, J. Chem. Phys. **117**, 9630 (2002).
[11]D. R. Kanis, M. A. Ratner, and T. J. Marks, Chem. Rev. **94**, 195 (1994).
[12]J. J. Wolff and R. Wortmann, in *Advances in Physical Organic Chemistry* (Academic Press Ltd, London, 1999), Vol. 32, p. 121.
[13]S. R. Marder, D. N. Beratan, and L. T. Cheng, Science **252**, 103 (1991).
[14]S. R. Marder, C. B. Gorman, B. G. Tiemann, and L. T. Cheng, J. Am. Chem. Soc. **115**, 3006 (1993).
[15]S. R. Marder, L. T. Cheng, B. G. Tiemann, A. C. Friedli, M. Blanchardde-sce, J. W. Perry, and J. Skindhoj, Science **263**, 511 (1994).
[16]M. Barzoukas and M. Blanchard-Desce, in *Advances in Multi-Photon Processes and Spectroscopy*, edited by S. H. Lin (World Scientific, Singapore, 2001), p. 261.
[17]M. Ferrero, M. Rerat, B. Kirtman, and R. Dovesi, J. Chem. Phys. **129**, 244110 (2008).
[18]M. Ferrero, B. Civalleri, M. Rerat, R. Orlando, and R. Dovesi, J. Chem. Phys. **131**, 214704 (2009).
[19]R. Orlando, V. Lacivita, R. Bast, and K. Ruud, J. Chem. Phys. **132**, 244106 (2010).
[20]S. Draguta, M. S. Fonari, A. E. Masunov, J. Zazueta, S. Sullivan, M. Y. Antipin, and T. V. Timofeeva, CrystEngComm **15**, 4700 (2013).
[21]A. Putrino, D. Sebastiani, and M. Parrinello, J. Chem. Phys. **113**, 7102 (2000).
[22]D. S. Chemla, J. L. Oudar, and J. Jerphagnon, Phys. Rev. B **12**, 4534 (1975).
[23]J. Zyss and J. L. Oudar, Phys. Rev. A **26**, 2028 (1982).
[24]A. I. Kitaigorodsky, *Molecular Crystals and Molecules* (Academic Press, Orlando, FL, 1973).
[25]T. V. Timofeeva, K. Y. Suponitsky, B. H. Cardelino, and R. D. Clark, Proc. SPIE **3796**, 229 (1999).
[26]L. N. Puntus, K. A. Lyssenko, M. Y. Antipin, and J. C. G. Bunzli, Inorg. Chem. **47**, 11095 (2008).
[27]J. Zyss and G. Berthier, J. Chem. Phys. **77**, 3635 (1982).
[28]H. Umezawa, S. Okada, H. Oikawa, H. Matsuda, and H. Nakanishi, Bull. Chem. Soc. Jpn. **80**, 1413 (2007).
[29]D. H. Bale, B. E. Eichinger, W. K. Liang, X. S. Li, L. R. Dalton, B. H. Robinson, and P. J. Reid, J. Phys. Chem. B **115**, 3505 (2011).
[30]B. F. Levine and G. C. Bethea, J. Chem. Phys. **65**, 2429 (1976).
[31]H. Reis, J. Chem. Phys. **125**, 014506 (2006).

[32] K. Y. Suponitsky, S. Tafur, and A. E. Masunov, J. Chem. Phys. **129**, 044109 (2008).
[33] Y. Q. Tu, Y. Luo, and H. Agren, J. Phys. Chem. B **109**, 16730 (2005).
[34] F. Terenziani, O. Mongin, C. Katan, B. K. G. Bhatthula, and M. Blanchard-Desce, Chem.-Eur. J. **12**, 3089 (2006).
[35] F. Terenziani, S. Ghosh, A. C. Robin, P. K. Das, and M. Blanchard-Desce, J. Phys. Chem. B **112**, 11498 (2008).
[36] Y. Liao, K. A. Firestone, S. Bhattacharjee, J. D. Luo, M. Haller, S. Hau, C. A. Anderson, D. Lao, B. E. Eichinger, B. H. Robinson, P. J. Reid, A. K. Y. Jen, and L. R. Dalton, J. Phys. Chem. B **110**, 5434 (2006).
[37] S. Yokoyama, T. Nakahama, A. Otomo, and S. Mashiko, J. Am. Chem. Soc. **122**, 3174 (2000).
[38] Y. Okuno, S. Yokoyama, and S. Mashiko, J. Phys. Chem. B **105**, 2163 (2001).
[39] E. Brouyere, A. Persoons, and J. L. Bredas, J. Phys. Chem. A **101**, 4142 (1997).
[40] A. Datta, F. Terenziani, and A. Painelli, Chemphyschem **7**, 2168 (2006).
[41] G. P. Bartholomew, I. Ledoux, S. Mukamel, G. C. Bazan, and J. Zyss, J. Am. Chem. Soc. **124**, 13480 (2002).
[42] I. V. Fedyanin, K. A. Lyssenko, N. V. Vorontsova, V. I. Rozenberg, and M. Y. Antipin, Mendeleev Commun. **13**, 15 (2003) .
[43] A. Bahl, W. Grahn, S. Stadler, F. Feiner, G. Bourhill, C. Brauchle, A. Reisner, and P. G. Jones, Angew. Chem., Int. Ed. Engl. **34**, 1485 (1995).
[44] M. Ronchi, M. Pizzotti, A. O. Biroli, S. Righetto, R. Ugo, P. Mussini, M. Cavazzini, E. Lucenti, M. Salsa, and P. Fantucci, J. Phys. Chem. C **113**, 2745 (2009).
[45] X. H. Zhou, J. D. Luo, S. Huang, T. D. Kim, Z. W. Shi, Y. J. Cheng, S. H. Jang, D. B. Knorr, R. M. Overney, and A. K. Y. Jen, Adv. Mater. **21**, 1976 (2009).
[46] D. Cornelis, E. Franz, I. Asselberghs, K. Clays, T. Verbiest, and G. Koeckelberghs, J. Am. Chem. Soc. **133**, 1317 (2011).
[47] T. Yasukawa, T. Kimura, and M. Uda, Chem. Phys. Lett. **169**, 259 (1990).
[48] S. Dibella, M. A. Ratner, and T. J. Marks, J. Am. Chem. Soc. **114**, 5842 (1992).
[49] R. S. Rowland and R. Taylor, J. Phys. Chem. **100**, 7384 (1996).
[50] T. Hamada, J. Phys. Chem. **100**, 8777 (1996).
[51] P. C. Ray and J. Leszczynski, Chem. Phys. Lett. **419**, 578 (2006).
[52] S. Thomas, Y. A. Pati, and S. Ramasesha, Cryst. Growth Des. **11**, 1846 (2011).
[53] M. Y. Balakina and O. D. Fominykh, Int. J. Quantum Chem. **108**, 2678 (2008).
[54] V. Moliner, P. Escribano, and E. Peris, New J. Chem. **22**, 387 (1998).
[55] R. W. Gora, R. Zalesny, A. Zawada, W. Bartkowiak, B. Skwara, M. G. Papadopoulos, and D. L. Silva, J. Phys. Chem. A **115**, 4691 (2011).
[56] J. Sarma, J. L. Rao, and K. Bhanuprakash, Chem. Mater. **7**, 1843 (1995).
[57] H. S. Nalwa, T. Watanabe, and S. Miyata, in *Nonlinear Optics of Organic Molecules and Polymers*, edited by H. S. Nalwa and S. Miyata (CRC, Boca Raton, 1997), p. 89.
[58] B. Champagne and D. M. Bishop, Adv. Chem. Phys. **126**, 41 (2003).
[59] F. Castet, B. Champagne, M. Nakano, and H. Takahashi, in *Computational Methods in Science and Engineering. Theory and Computation: Old Problems and New Challenges*, edited by G. Maroulis and T. Simos (American Institute of Physics, 2007), Vol. 1, p. 350.
[60] B. Skwara, R. W. Gora, and W. Bartkowiak, Chem. Phys. Lett. **406**, 29 (2005).
[61] B. Skwara, W. Bartkowiak, A. Zawada, R. W. Gora, and J. Leszczynski, Chem. Phys. Lett. **436**, 116 (2007).
[62] K. Y. Suponitsky, V. G. Tsirelson, and D. Feil, Acta Crystallogr. **55**, 821 (1999).
[63] J. Perez and M. Dupuis, J. Phys. Chem. **95**, 6525 (1991).
[64] K. C. Wu, J. G. Snijders, and C. S. Lin, J. Phys. Chem. B. **106**, 8954 (2002).
[65] M. Olejniczak, M. Pecul, B. Champagne, and E. Botek, J. Chem. Phys. **128**, 244713 (2008).
[66] M. Guillaume, E. Botek, B. Champagne, F. Castet, and L. Ducasse, J. Chem. Phys. **121**, 7390 (2004).
[67] M. Guillaume, E. Botek, B. Champagne, F. Castet, and L. Ducasse, Int. J. Quantum Chem. **90**, 1378 (2002).
[68] F. Castet and B. Champagne, J. Phys. Chem. A **105**, 1366 (2001).
[69] B. Skwara, W. Bartkowiak, and J. Leszczynski, Struct. Chem. **15**, 363 (2004).
[70] L. Turi and J. J. Dannenberg, Chem. Mater. **6**, 1313 (1994).
[71] J. J. Dannenberg, L. Haskamp, and A. Masunov, J. Phys. Chem. A **103**, 7083 (1999).
[72] A. Masunov and J. J. Dannenberg, J. Phys. Chem. B **104**, 806 (2000).
[73] L. Turi and J. J. Dannenberg, J. Phys. Chem. **97**, 12197 (1993).
[74] L. Turi and J. J. Dannenberg, J. Am. Chem. Soc. **116**, 8714 (1994).
[75] L. Turi and J. J. Dannenberg, J. Phys. Chem. **100**, 9638 (1996).
[76] J. J. Dannenberg, J. Mol. Struct. **615**, 219 (2002).
[77] H. J. Song, H. M. Xiao, and H. S. Dong, J. Chem. Phys. **125**, 074308 (2006).
[78] A. S. Ozen, P. Doruker, and V. Aviyente, J. Phys. Chem. A **111**, 13506 (2007).
[79] G. Fradelos, J. W. Kaminski, T. A. Wesolowski, and S. Leutwyler, J. Phys. Chem. A **113**, 9766 (2009).
[80] B. Champagne, E. A. Perpete, S. J. A. van Gisbergen, E. J. Baerends, J. G. Snijders, C. Soubra-Ghaoui, K. A. Robins, and B. Kirtman, J. Chem. Phys. **109**, 10489 (1998).
[81] B. Champagne, E. A. Perpete, D. Jacquemin, S. J. A. van Gisbergen, E. J. Baerends, C. Soubra-Ghaoui, K. A. Robins, and B. Kirtman, J. Phys. Chem. A **104**, 4755 (2000).
[82] N. Matsuzawa and D. A. Dixon, J. Phys. Chem. **98**, 2545 (1994).
[83] A. J. Cohen, N. C. Handy, and D. J. Tozer, Chem. Phys. Lett. **303**, 391 (1999).
[84] Y. Zhao and D. G. Truhlar, J. Phys. Chem. A **110**, 13126 (2006).
[85] Y. Zhao and D. G. Truhlar, Theor. Chem. Acc. **120**, 215 (2008).
[86] Y. Zhao and D. G. Truhlar, Acc. Chem. Res. **41**, 157 (2008).
[87] L. De Boni, C. Toro, A. E. Masunov, and F. E. Hernandez, J. Phys. Chem. A **112**, 3886 (2008).
[88] I. A. Mikhailov, K. D. Belfield, and A. E. Masunov, J. Phys. Chem. A **113**, 7080 (2009).
[89] I. A. Mikhailov, M. V. Bondar, K. D. Belfield, and A. E. Masunov, J. Phys. Chem. C **113**, 20719 (2009).
[90] I. A. Mikhailov, S. Tafur, and A. E. Masunov, Phys. Rev. A **77**, 012510 (2008).
[91] P. D. Patel and A. E. Masunov, J. Phys. Chem. A **113**, 8409 (2009).
[92] P. D. Patel, I. A. Mikhailov, K. D. Belfield, and A. E. Masunov, Int. J. Quantum Chem. **109**, 3711 (2009).
[93] D. Bokhan and R. J. Bartlett, J. Chem. Phys. **127**, 174102 (2007).
[94] C. M. Isborn, A. Leclercq, F. D. Vila, L. R. Dalton, J. L. Bredas, B. E. Eichinger, and B. H. Robinson, J. Phys. Chem. A **111**, 1319 (2007).
[95] P. Salek, O. Vahtras, J. D. Guo, Y. Luo, T. Helgaker, and H. Agren, Chem. Phys. Lett. **374**, 446 (2003).
[96] P. Salek, T. Helgaker, O. Vahtras, H. Agren, D. Jonsson, and J. Gauss, Mol. Phys. **103**, 439 (2005).
[97] M. de Wergifosse and B. Champagne, J. Chem. Phys. **134**, 074113 (2011).
[98] T. Yanai, D. P. Tew, and N. C. Handy, Chem. Phys. Lett. **393**, 51 (2004).
[99] O. A. Vydrov, G. E. Scuseria, J. P. Perdew, A. Ruzsinszky, and G. I. Csonka, J. Chem. Phys. **124**, 094108 (2006).
[100] H. Iikura, T. Tsuneda, T. Yanai, and K. Hirao, J. Chem. Phys. **115**, 3540 (2001).
[101] O. A. Vydrov, J. Heyd, A. V. Krukau, and G. E. Scuseria, J. Chem. Phys. **125**, 074106 (2006).
[102] O. A. Vydrov and G. E. Scuseria, J. Chem. Phys. **125**, 234109 (2006).
[103] A. Ruzsinszky, J. P. Perdew, G. I. Csonka, O. A. Vydrov, and G. E. Scuseria, J. Chem. Phys. **125**, 194112 (2006).
[104] J. Heyd, G. E. Scuseria, and M. Ernzerhof, J. Chem. Phys. **118**, 8207 (2003).
[105] M. Kamiya, H. Sekino, T. Tsuneda, and K. Hirao, J. Chem. Phys. **122**, 234111 (2005).
[106] H. Sekino, Y. Maeda, M. Kamiya, and K. Hirao, J. Chem. Phys. **126**, 014107 (2007).
[107] D. Jacquemin, E. A. Perpete, M. Medved, G. Scalmani, M. J. Frisch, R. Kobayashi, and C. Adamo, J. Chem. Phys. **126**, 191108 (2007).
[108] E. A. Perpete, D. Jacquemin, C. Adamo, and G. E. Scuseria, Chem. Phys. Lett. **456**, 101 (2008).
[109] B. Kirtman, S. Bonness, A. Ramirez-Solis, B. Champagne, and H. Matsumoto, H. Sekino, J. Chem. Phys. **128**, 114108 (2008).
[110] L. Ferrighi, L. Frediani, C. Cappelli, P. Salek, H. Agren, T. Helgaker, and K. Ruud, Chem. Phys. Lett. **425**, 267 (2006).
[111] M. J. G. Peach, P. Benfield, T. Helgaker, and D. J. Tozer, J. Chem. Phys. **128**, 044118 (2008).
[112] D. Jacquemin, E. A. Perpete, G. Scalmani, M. J. Frisch, R. Kobayashi, and C. Adamo, J. Chem. Phys. **126**, 144105 (2007).
[113] D. Jacquemin, E. A. Perpete, I. Ciofini, and C. Adamo, J. Comput. Chem. **29**, 921 (2008).
[114] P. A. Limacher, K. V. Mikkelsen, and H. P. Luthi, J. Chem. Phys. **130**, 194114 (2009).

[115]H. Fukui, Y. Inoue, R. Kishi, Y. Shigeta, B. Champagne, and M. Nakano, Chem. Phys. Lett. **523**, 60 (2012).
[116]R. Kishi, S. Bonness, K. Yoneda, H. Takahashi, M. Nakano, E. Botek, B. Champagne, T. Kubo, K. Kamada, K. Ohta, and T. Tsuneda, J. Chem. Phys. **132**, 094107 (2010).
[117]V. Polo, J. Grafenstein, E. Kraka, and D. Cremer, Chem. Phys. Lett. **352**, 469 (2002).
[118]V. Polo, E. Kraka, and D. Cremer, Theor. Chem. Acc. **107**, 291 (2002).
[119]V. Polo, E. Kraka, and D. Cremer, Mol. Phys. **100**, 1771 (2002).
[120]K. Y. Suponitsky, A. E. Masunov, and M. Y. Antipin, Mendeleev Commun. **18**, 265 (2008).
[121]K. Y. Suponitsky, A. E. Masunov, and M. Y. Antipin, Mendeleev Commun. **19**, 311 (2009).
[122]K. Y. Suponitsky, Y. Liao, and A. E. Masunov, J. Phys. Chem. A **113**, 10994 (2009).
[123]Y. Zhao, N. E. Schultz, and D. G. Truhlar, J. Chem. Theory Comput. **2**, 364 (2006).
[124]Y. Zhao and D. G. Truhlar, J. Chem. Theory Comput. **3**, 289 (2007).
[125]H. R. Leverentz and D. G. Truhlar, J. Phys. Chem. A **112**, 6009 (2008).
[126]J. Sponer, K. E. Riley, and P. Hobza, Phys. Chem. Chem. Phys. **10**, 2595 (2008).
[127]M. J. Frisch, G. W. Trucks, H. B. Schlegel *et al*., Gaussian 03, Revision E.01, Gaussian, Inc., Wallingford, CT, 2004.
[128]A. E. Reed, R. B. Weinstock, and F. Weinhold, J. Chem. Phys. **83**, 735 (1985).
[129]A. E. Reed, L. A. Curtiss, and F. Weinhold, Chem. Rev. **88**, 899 (1988).
[130]K. Sutter, C. Bosshard, M. Ehrensperger, P. Gunter, and R. J. Twieg, IEEE J. Quantum Electron. **24**, 2362 (1988).
[131]R. Morita and P. V. Vidakovic, Appl. Phys. Lett. **61**, 2854 (1992).
[132]See supplementary material at http://dx.doi.org/10.1063/1.4819265 for Figures 1S–7S and Tables 1S–8S.
[133]P. V. Vidakovic, M. Coquillay, and F. Salin, J. Opt. Soc. Am. B **4**, 998 (1987).
[134]F. H. Allen, Acta Crystallogr. **58**, 380 (2002).
[135]K. Y. Suponitsky, K. A. Lyssenko, and M. Y. Antipin, personal communication (2001).
[136]E. G. McRae and M. Kasha, J. Chem. Phys. **28**, 721 (1958).
[137]V. V. Egorov and M. V. Alfimov, Phys. Usp. **50**, 985 (2007).
[138]B. I. Shapiro, Usp. Khim. **75**, 433 (2006).
[139]J. Applequist, J. R. Carl, and K. K. Fung, J. Am. Chem. Soc. **94**, 2952 (1972).
[140]M. Guillaume, B. Champagne, D. Begue, and C. Pouchan, J. Chem. Phys. **130**, 134715 (2009).
[141]M. B. Kanoun, E. Botek, and B. Champagne, Chem. Phys. Lett. **487**, 256 (2010).
[142]M. B. Kanoun and B. Champagne, Int. J. Quantum Chem. **111**, 880 (2011).
[143]A. Segerie, F. Castet, M. B. Kanoun, A. Plaquet, V. Liegeois, and B. Champagne, Chem. Mater. **23**, 3993 (2011).
[144]B. Champagne, D. Jacquemin, J. M. Andre, and B. Kirtman, J. Phys. Chem. A **101**, 3158 (1997).